RESEARCH PAPER

Application of PSO and Curve Fitting for the Optimization of Compact L-Shaped Open Ended Slot Loaded Rectangular Patch Antenna

Ramesh Kumar Verma[1]

Abstract

This paper demonstrates an application of PSO (particle swarm optimization) for bandwidth optimization of L-shaped open ended slot antenna. An L-shaped open ended slot antenna design (non-optimized) has been optimized by MATLAB-based PSO for bandwidth enhancement at frequency 2.50 GHz. Various parameters of L-shaped open ended slot antenna have been changed one by one at a time for generating the data for bandwidth and resonant frequency. These data has been used in Graphmatica software (Curve fitting) for generating curve and relationship equations. Finally, the performance of PSO optimized L-shaped open ended slot antenna has been executed and the achievement is compared with non-optimized L-shaped open ended slot antenna. The bandwidth of microstrip line feed optimized L-shaped open ended slot antenna has been increased by 43.86% (from 30.8 to 44.31%) as compared to non-optimized L-shaped open ended slot antenna keeping resonant frequency exactly at desired design frequency 2.50 GHz. Optimized antenna performance is verified by the close agreement between measured and simulated results.

Keywords PSO (Particle swarm optimization) · L-shaped · Bandwidth · Graphmatica · MATLAB

1 Introduction

Advances in wireless communication devices have increased the need for compact as well as low-profile antennas exhibiting high gain along with wide bandwidth. Microstrip antenna (MSA) offers heap of merits like light weight, compactness and low profile. However, the major weakness of MSA is its narrow bandwidth, smaller gain, low efficiency and spurious feed radiation. There are many substrate materials which can be utilized to design MSA having dielectric constant between 2.2 and 12 (Balanis 2005). The material having smaller value of dielectric constant yields better efficiency and larger bandwidth. The bandwidth of MSA can be expanded by utilizing several techniques, for example, considering different kinds of patch configuration, creating different types of notches and slots in antenna patch. The geometry of antenna design

have a strip of conductive surface called patch which is generated on the top layer of dielectric material separated by another conductive layer known as ground layer which lies on bottom surface of dielectric material. Design technique of a microstrip antenna is a planar technique which can create waves and lines conveying signals. These radiated waves and line signals are coupled by antennas.

The size of antenna is excessively essential for wireless conversation systems. With the decrease in antenna size, bandwidth also decreases and these aspects restrict the designing of compact antennas (Sun et al. 2017). The antenna bandwidth is increased by extending the length of electrical path of antenna by optimizing the shape of patch (Wang and Lancaster 1999). Kennedy and Eberhart have been interpreting the PSO optimization theory for nonlinear functions (Kennedy and Eberhart 1995). An optimization method has been presented for gap coupled rectangular MSA between 3 and 18 GHz frequency using PSO algorithm (Dey et al. 2016). However, modified PSO has been executed followed by MATLAB and IE3D on a traditionally optimized broad band antenna showing bandwidth enhancement of 12% with size reduction of 20.84% (Kibria et al. 2014). Another optimized antenna of butterfly-shape

✉ Ramesh Kumar Verma
ramesh85.ec@gmail.com

[1] Department of Electronics and Communication Engineering, Bundelkhand Institute of Engineering and Technology, Jhansi, UP, India

Ⓐ Springer

exhibiting 40.1% bandwidth has been designed and optimized using PSO for wireless and RFID applications (Sun et al. 2016). An optimization of swastika shape (Kaur et al. 2017a) and PSI (Ψ) shape (Kaur et al. 2017b) slotted fractal antenna of multiband have been presented using ANN, genetic and Bat algorithm exhibiting total bandwidth of 215.98 MHz and 696.24 MHz, respectively. Another optimization-based fractal antenna (Gupta et al. 2020) also presented with the help of modified BP-PSO (bacterial foraging-PSO) for bandwidth enhancement only 34%. Jin and Samii design and optimized both multiband as well as wideband antenna (Jin and Samii 2005) using PSO along with FDTD (finite-difference time-domain) algorithm exhibiting bandwidth of 30.5% (640 MHz). Islam et al. (Islam et al. 2009) have been presented an optimization of MSA exhibiting 15% bandwidth increment having inverted E-shape patch using PSO. Behera and Choukiker have been presented a dual band inset feed MSA design and optimization methods (Behera and Choukiker 2010). PSO exhibits bandwidth of 33.54 MHz between 2.383 and 2.417 GHz. Choukiker et al. (Choukiker et al. 2011) have been proposed the geometry of E-shape patch antenna using inset-fed and optimized with particle swarm optimization (PSO) technique to achieve bandwidth of 121.9 MHz for ISM band operation between 2.40 and 2.52 GHz. Moreover, a slot loaded dual band PSO optimized MSA has been designed with circular shape patch (Tiang et al. 2014). Another MSA of I-shape patch has been presented to enhance the bandwidth by using PSO optimization carried out by curve fitting (Rajpoot et al. 2014). A wideband and compact 3D-printed hemispherical antenna (Tang et al. 2018) having bandwidth 127 MHz (16.87%) has been proposed using PSO. An antenna of W-shape patch consisting a pair of V-shape slots for enhancing bandwidth has been proposed using fuzzy-based GA (Neyestanak et al. 2007). Kamakshi et al. (Kamakshi et al. 2014) have been designed a broadband antenna with one slot and three notches for bandwidth enhancement. Furthermore, a dual feed U-shape slotted broadband antenna (He et al. 2015) and a wideband antenna of stub loaded annular sector dipole (Zhang et al. 2016) have been designed. However, a circular shape slotted antenna (Sukur et al. 2016) has been proposed for enhancing bandwidth. Aneesh et al. (Aneesh et al. 2013) proposed an analysis of S-shape microstrip patch antenna of bandwidth 21.62% theoretical and 20.49% simulated for bluetooth application. Due to narrow bandwidth of MSA, it becomes very essential for designing of MSA to accurately match its resonant frequency at design frequency. In a narrow band region, an antenna can only perform efficiently at resonant frequency. Thus a technique becomes more useful in antenna designing that matched the resonant frequency and enhance the antenna bandwidth.

In this proposed method, the bandwidth of MSA has been increased by optimization of patch parameters using PSO. Application of PSO and curve fitting along with MATLAB (MATLAB Version 2014a) is investigated to optimize the design of L-shaped open ended slot antenna. Graphmatica software (Graphmatica 2014) and IE3D simulation tool (Zeland Software 2012) has been used for curve fitting (Generating relationship equation) and antenna simulation respectively and while MATLAB is used for optimization. The proposed optimized L-shaped open ended slot antenna has been fabricated by utilizing low cost and easily available FR-4 substrate (glass epoxy) at 2.50 GHz frequency for WLAN/WiMAX applications (Zhang et al. 2016).

The content of proposed article is organized in following sections. The antenna design specification and geometry are presented in Sects. 2 and 3, respectively. Sections 4 and 5 presents the design of conventional antenna and non-optimized L-shaped open ended slot antenna. PSO algorithm and optimization procedure are discussed in Sect. 6 and Sect. 7, respectively. The results discussion, experimental validation and comparative performance investigation of proposed antenna are presented in Sect. 8. Finally, the conclusion remark of proposed antenna is discussed in Sect. 9.

2 Antenna Design Specification for Conventional Antenna

The proposed structure of antenna is designed by using FR-4 substrate (glass epoxy) of thickness 1.6 mm, dielectric constant 4.4 and loss tangent 0.02 at 2.50 GHz frequency. Flow chart for step by step design of antenna and optimization is shown in Fig. 1. The patch of antenna is excited by 50Ω microstrip line feed. Using IE3D simulation software, design and simulation work has been performed.

For an antenna design, the width (W) and length (L) of a rectangular shape patch is calculated by Eq. (1) and Eqs. (2–4), respectively (Balanis 2005).
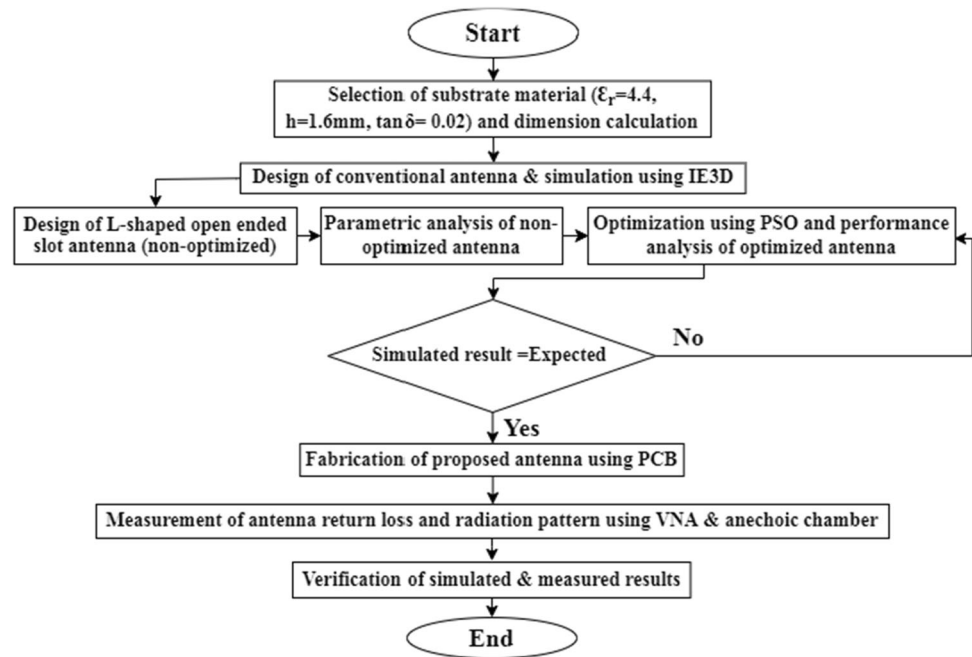
$$W = \frac{c}{2f_r} \sqrt{\frac{2}{\varepsilon_r + 1}} \qquad (1)$$

where $c = 3 \times 10^8$ ms^{-1} in air (speed of light), $f_r = 2.50$ GHz (design frequency), $\varepsilon_r = 4.4$ (substrate dielectric constant).

Effective dielectric constant ($\varepsilon_{\text{reff}}$) of the substrate is given below as (Balanis 2005).

$$\varepsilon_{reff} = \frac{\varepsilon_r + 1}{2} + \frac{\varepsilon_r - 1}{2}\left(1 + \frac{12h}{W}\right)^{-\frac{1}{2}} \qquad (2)$$

Fig. 1 Systematic design steps of proposed structure

Extension length of patch (ΔL) is calculated by (Balanis 2005).

$$\frac{\Delta L}{h} = 0.412 \frac{\left(\varepsilon_{reff} + 0.30\right)\left(\frac{W}{h} + 0.264\right)}{\left(\varepsilon_{reff} - 0.258\right)\left(\frac{W}{h} + 0.8\right)} \tag{3}$$

Finally, the following equation given below can be used to calculate the absolute patch length value as (Balanis 2005).

$$L = \frac{c}{2f_r\sqrt{\varepsilon_{reff}}} - 2\Delta L \tag{4}$$

The length and width of the patch calculated by Eqs. (1–4) is L = 28.2 mm (Lp) and W = 36.5 mm (Wp), respectively. Length and width of ground layer can be calculated by equation given below as (Verma and Srivastava 2020).

$$L_g = 6h + L_p \tag{5}$$

$$W_g = 6h + W_p \tag{6}$$

The length (Lg) and width (Wg) of the ground layer are 37.8 mm and 46.1 mm, respectively, evaluated by Eqs. (5) and (6).

3 Proposed Antenna Geometry

The detailed optimized antenna geometry (front and side view) has been exhibited in Fig. 2a and b, respectively. Antenna is designed on a ground layer ($Lg \times Wg$) of size 37.8 mm × 46.1 mm ($0.32\lambda_0 \times 0.38\lambda_0 = 0.12\ \lambda_0^2$) at frequency 2.50 GHz. The ground plane of proposed antenna is considered at co-ordinate (0, 0) from bottom left corner of antenna. The radiating patch of antenna ($Lp \times Wp$) has size 28.2 mm × 36.5 mm ($0.24\lambda_0 \times 0.30\lambda_0$). The patch of antenna is fed by microstrip line feed of 50Ω connected at left bottom corner at coordinate (2.35, 8.22) via a feed strip of optimized length (L_2) and width (W_2) of 2.45 mm and 6.84 mm, respectively. The optimized dimensions of proposed antenna are shown in Table 1.

4 Conventional Antenna Design

The radiating patch (28.2 mm × 36.5 mm) of conventional antenna is designed on a ground plane of size 37.8 mm × 46.1 mm. Initially, microstrip line feed (50Ω) is connected at bottom left corner of patch via a feed strip of length L_2 = 3 mm and width W_2 = 5 mm. The design of conventional antenna is exhibited in Fig. 3a. The conventional antenna is designed and simulated by IE3D simulation software for 1 GHz to 3 GHz. The fractional bandwidth of conventional antenna is obtained 13.93% (340 MHz) between 2.27 and 2.61 GHz resonating at frequency 2.44 GHz with a poor return loss of − 12.96 dB. The VSWR value of conventional antenna is obtained 1.58 at resonant frequency 2.44 GHz. Return loss graph against frequency of conventional antenna is exhibited in Fig. 4.
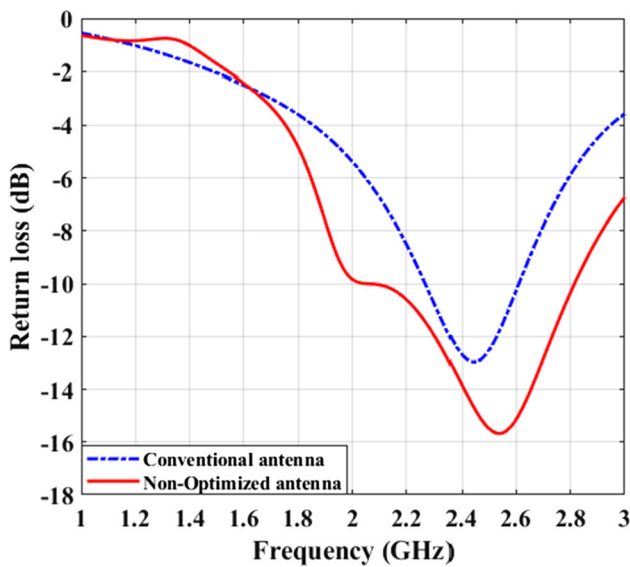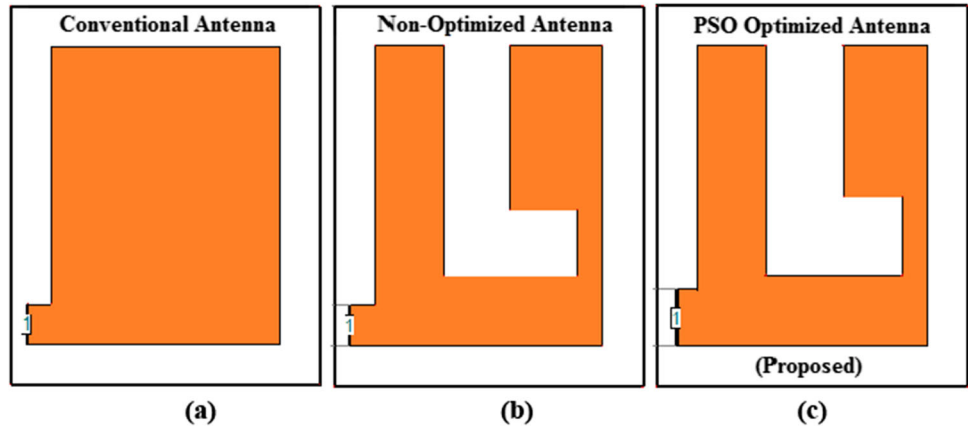
Fig. 2 Antenna geometry **a** Optimized L-shaped open ended slot antenna, **b** Side view **c** Prototype antenna design (front view) and **d** Bottom view

(a)

(b)

(c)

(d)
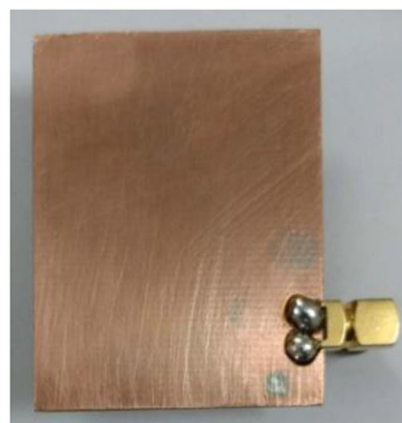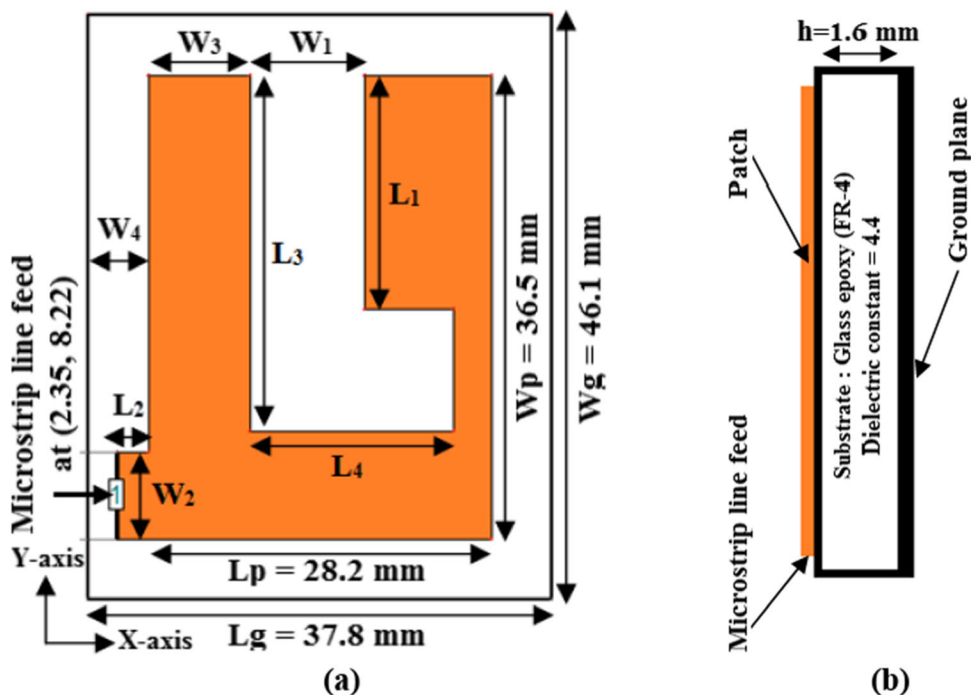
Table 1 Optimized dimensional and basic parameters of proposed antenna

Parameters	Value (mm)	Parameters	Value
Patch length (Lp)	28.2	Frequency (f_r)	2.50 GHz
Patch width (Wp)	36.5	Dielectric constant (ε_r)	4.4
Ground plane length (Lg)	37.8	Substrate thickness (h)	1.6 mm
Ground plane width (Wg)	46.1	Speed of light (c)	3×10^8 ms^{-1}
Vertical arm length of L-slot (L_1)	18.42	Loss tangent ($tan\delta$)	0.02
Vertical arm width of L-slot (W_1)	9.04	Line feed	50 Ω
Feed strip length (L_2)	2.45	Feed position	(2.35, 8.22)
Feed strip width (W_2)	6.84		

Fig. 3 Antenna growth
a Conventional patch antenna
b L-shaped open ended slot antenna and **c** PSO optimized L-shaped open ended slot antenna

Fig. 4 Return loss plot of conventional and L-shaped open ended slot antenna (Non-Optimized)

Table 2 Parameters of L-shaped open ended slot antenna (non-optimized)

Parameters	Values (mm)
Vertical arm length (L_1)	20
Vertical arm width (W_1)	8
Vertical arm length (L_3)	28
Horizontal arm length (L_4)	16
Horizontal arm length ($L_4 - W_1$)	8
Horizontal arm width ($L_3 - L_1$)	8

The non-optimized L-shaped open ended slot antenna is also designed and simulated by IE3D software between 1 to 3 GHz. The maximum bandwidth of L-shaped open ended slot antenna has been obtained 30.8% (750 MHz) between 2.06 and 2.81 GHz resonating at 2.54 GHz resonant frequency with -15.67 dB return loss for same feed length 3 mm and width 5 mm. Comparative return loss plot of L-shaped open ended slot antenna with conventional antenna has been exhibited in Fig. 4.

It can be noticed that, fractional bandwidth of L-shaped open ended slot antenna is increased from 13.93 to 30.8%. Return loss also improved from -12.96 dB to -15.67 dB. VSWR of L-shaped open ended slot antenna is observed 1.39 at resonant frequency 2.54 GHz. The above recorded fractional bandwidth (30.8%) and resonant frequency (2.54 GHz) of L-shaped open ended slot antenna are the main intention of optimization technique to enhanced bandwidth (BW) by changing variable parameters of antenna while keeping resonant frequency (FR) of 2.54 GHz near to design frequency 2.50 GHz.

5 L-shaped Open-Ended Slot Antenna Design

The geometry of L-shaped open ended slot antenna (non-optimized) has been obtained by etching a vertical rectangular slot of size $L_1 \times W_1 = 20$ mm $\times$ 8 mm and a horizontal rectangular slot of size $L_4 \times (L_3 - L_1)$ $= 16$ mm $\times$ 8 mm as exhibited in Fig. 3b. Geometrical parameter $L_3 = 28$ mm, $L_4 = 16$ mm, $W_3 = 8.6$ mm and $W_4 = 4.8$ mm are fixed while slot parameter L_1, W_1 and feed strip parameter L_2, W_2 has been considered as variable. Initial values of variable parameters L_1, L_2, W_1 and W_2 are 20 mm, 3 mm, 8 mm and 5 mm, respectively. The resonant frequency and bandwidth of antenna can be optimized by adjusting these selected parameters. All dimensional parameters of L-shaped open ended slot antenna are exhibited in Table 2.

6 PSO Algorithm

Eberhart and Kennedy described the first basic idea of PSO (Particle swarm optimization) in year 1995 inspired by social behavior of bird flocking or fish schooling for

solving optimization problem based on population (Kennedy and Eberhart 1995). PSO is iteration-based computational optimization method that optimized an issue by enhancing candidate solution. The PSO algorithm-based optimization issues are solved by candidate solution considered as particle and generated population considered as swarm. These particles are moved all over in search space by following current optimal particle using simple mathematical equations with both velocity and particle position. In overall search space, each particle's movement is governed by the direction of the most outstanding location, known location of best local as well as better current location acquired by the new particle. The swarm movement is predicted to approach in the direction of the best options. Because the whole process is automatically repeated, it is assumed but not guaranteed that an appropriate solution will be identified at some point. As a result, throughout the searching region, movement of particles are always supervised in the direction of individual best called personal best (pbest) and entire group best known position called global best (gbest) (Islam et al. 2009). To determine the current position of particle, a mathematical equation is used for velocity updating (Tiang et al. 2014).

$$V_i(t+1) = W * V_i(t) + \lambda_1 * \delta_1 * (X_{pbest}(t) - X_i(t)) + \lambda_2 * \delta_2 * (X_{gbest}(t) - X_i(t))$$

(7)

where $V_i(t)$: Particle velocity in ith measurement. $X_i(t)$: Particle coordinates in ith measurement. t: Current iteration. W: Weight coefficient which is time dependant and linearly decreases from 0.9 to 0.6 δ_1 and δ_2: Random functions apply to produces uniform distributed numbers lies between 0 and 1.

λ_1 and λ_2: Random constant, normally set at 2.0

At the end of iteration, current updated position of a particle is determined (Tiang et al. 2014) by Eq. (8).

$$X_i(t+1) = X_i(t) + V_i(t+1)$$

(8)

The weighting function (w) which is used in above Eqs. (7) is given by

$$w = w_{Max} - \frac{[(w_{Max} - w_{Min}) * Iter]}{MaxIter}$$

(9)

where w_{Max} = Initial weight, w_{Min} = Final weight, $Iter$ = Current iteration number and $MaxIter$ = Maximum iteration number.

The calculations are performed for each dimension of an N-dimensional optimization problem. The position of ith particle is recorded by X_{pbest} that attains self-personal best fitness value while the position attains among all for global best fitness value is recorded by X_{gbest}.

7 Optimization Application of PSO

The parameters of antenna patch (Table 3) which are selected for optimization like length and width of L-shape slot and feed strip generates particle position and in starting, select a set of such positions of particle. The value of fitness function for each individual particle position is evaluated by cost function and every generated cost function is a nonlinear function of particles position while rest antenna parameters are works as input set and required characteristics. Based on antenna characteristic, it may be single aim oriented like only antenna bandwidth or only antenna resonant frequency or multi aim oriented like both antenna bandwidth (BW) as well as resonating frequency (FR).

7.1 Parameters and Range of Variation

The parameter L_1 (Vertical arm length of L-shaped open ended slot), L_2 (Feed strip length), W_1 (Vertical arm width of L-shaped open ended slot) and W_2 (Feed strip width) are considered as variable parameter of antenna out of L_1, W_1, L_2, W_2, L_3, W_3, L_4 and W_4 for the purpose of optimization. One–one antenna using IE3D has been designed for all iterations and corresponding bandwidth, resonant frequency and return loss are recorded. The intention of the optimization technique to enhanced the bandwidth (BW) that is simulated above for L-shaped open ended slot antenna by varying these four variable parameters of patch one by one constantly at a time with in selected range of variation and rest three parameters are kept unchanged while keeping resonant frequency (FR) 2.54 GHz near desired frequency 2.50 GHz. The selected variable parameters and their range with step size of variation are shown in Table 3.

7.2 Variation of Parameter L₁

The parameter L_1 is changed from 15 to 25 mm in step of 1 mm. Initially, L_1 parameter was 20 mm. It generates total 11 different antennas and one antenna for L_1 = 20 mm is common. An antenna for L_1 = 24 mm shows maximum bandwidth of 35.16% (840 MHz) resonating between 1.97 and 2.81 GHz at 2.52 GHz resonant frequency with return loss of − 16.05 dB. Comparative return loss plot for each values of L_1 parameter is shown in Fig. 5a. Resonant frequencies of all generated antennas varies between 2.52 (L_1 = 25 mm) and 2.56 GHz (L_1 = 15 mm) while bandwidth varies from minimum bandwidth 24.95% (L_1 = 15 mm) to maximum bandwidth 35.16% (L_1 = 24 mm).

Table 3 Variation range of parameter and step size

Parameter (Initial value)	Lower limit (mm)	Upper limit (mm)	Step size variation (mm)
L_1 (20 mm)	15	25	1
W_1 (8 mm)	2	14	1
L_2 (3 mm)	1.8	4.2	0.2
W_2 (5 mm)	4.2	9	0.4
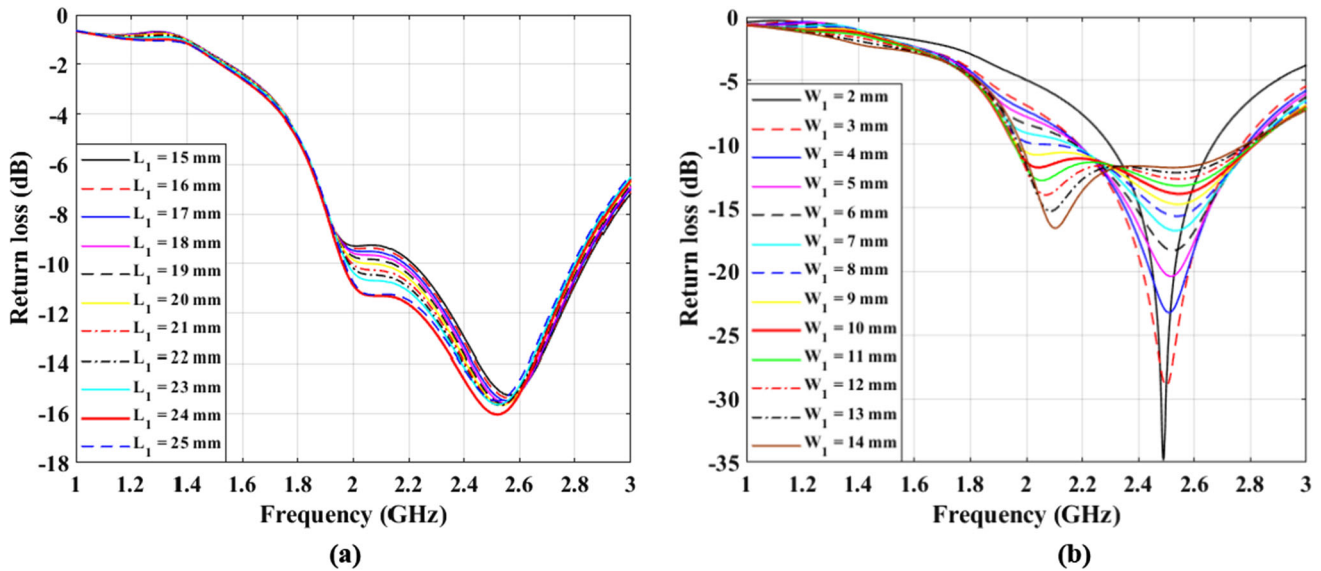
Fig. 5 Return loss plot at different values of **a** L_1 and **b** W_1

7.3 Variation of Parameter W_1

W_1 parameter also has been changed from 2 to 14 mm in step of 1 mm like parameter L_1. Initial value of W_1 parameter was 8 mm. Hence, total 13 different antennas containing one common antenna for W_1 = 8 mm has been generated. One antenna for W_1 = 10 mm out of 13 different antennas has maximum bandwidth 35.98% (860 MHz) between 1.96 and 2.82 GHz resonating at 2.55 GHz with return loss of − 13.91 dB. The bandwidth of all generated antennas lies between minimum bandwidth 14.89% (W_1 = 2 mm) and maximum bandwidth 35.98% (W_1 = 10 mm). Also resonant frequencies of all antennas varies between 2.07 (W_1 = 12 mm) and 2.55 GHz (W_1 = 11 mm). Comparative return loss plot has been shown in Fig. 5b.

7.4 Variation of Parameter L_2

L_2 parameter has been changed from 1.8 to 4.2 mm in step of 0.2 mm. Initial value of L_2 parameter was 3 mm. It also generate total 13 different antennas containing one common antenna for L_2 = 3 mm. The small step size of L_2 is taken because length of L_2 is very small and in such small range, available scope of step size is less. It has been

noticed that one antenna out of 13 antennas for L_2 = 2.2 mm shows maximum bandwidth 38.81% (900 MHz) between 1.91 and 2.83 GHz resonating at 2.45 GHz with return loss of − 20.73 dB. Resonant frequencies of all generated antennas varies between 2.38 GHz (L_2 = 1.8 mm) to 2.58 GHz (L_2 = 4.2 mm) while bandwidth varies from minimum bandwidth 15.2% (L_2 = 4.2 mm) to maximum bandwidth 38.81% (L_2 = 2.2 mm). Comparative return loss plot for each values of L_2 has been shown in Fig. 6a.

7.5 Variation of Parameter W_2

Initial value of W_2 parameter was 5 mm. For the observing the effect of W_2 parameter on antenna performance, it has been changed from 4.2 to 9 mm in step of 0.4 mm. A maximum bandwidth of 37.86% (920 MHz) of one antenna for W_2 = 8.2 mm out of 13 different antennas is obtained between 1.97 and 2.89 GHz resonating at 2.57 GHz with return loss of –18.55 dB. Antenna for W_2 = 5 mm is common in all 13 generated different antennas. Comparative return loss plot for each values of W_2 parameter is shown in Fig. 6(b). The bandwidth of all generated antennas lies between minimum bandwidth 18.55% (W_2 = 9 mm) and maximum bandwidth 37.86%
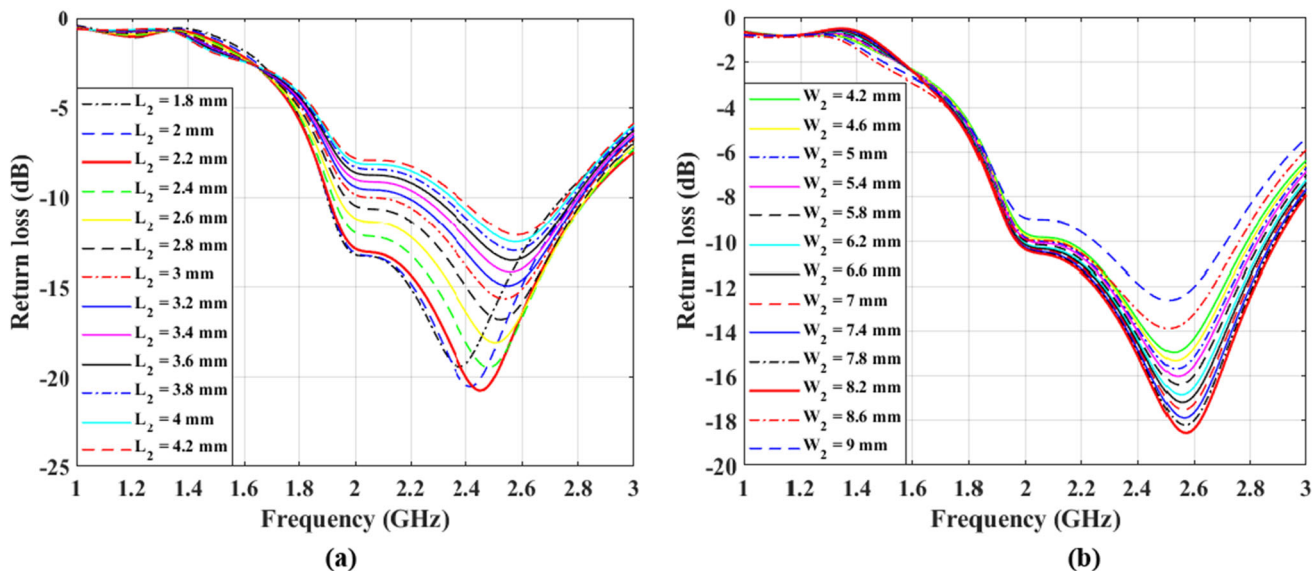
Fig. 6 Return loss plot at different values of **a** L_2 and **b** W_2

($W_2 = 8.2$ mm). Also resonant frequencies of all antennas varies between 2.51 ($W_2 = 9$ mm) and 2.57 GHz ($W_2 = 7.8$ mm).

7.6 Curve Fitting

Graphmatica tool (Curve fitting) is used to set up the relationship among L_1, L_2, W_1 and W_2 parameter to BW and FR individually. Each parameter is varied one by one constantly at a time with in selected range of variation and rest three parameters are kept unchanged. Parameter L_1 generates 11 different antennas while W_1, L_2 and W_2 generates separately 13–13 different antennas having one–one antenna (non-optimized) of L-shaped open ended slotted patch at their initial value is common in all parameters. Thus, total 47 (11 + 13 + 13 + 13–3) different antennas are available for analysis and generating cost function. Bandwidth (BW), resonant frequency (FR) and return loss (RL) are calculated for each antenna by IE3D simulation tool. Out of these antennas, only three-three antenna results for each variable parameter have been exhibited in Table 4. One antenna for lower limit and one antenna for upper limit of parameter and one antenna that have maximum bandwidth are shown.

The relationship equations between an individual parameter to bandwidth (BW) and resonant frequency (FR) have been formed by applying the generated data achieved from all antennas for each parameter in Graphmatica software (curve fitting). Similarly, it is also followed for rest selected parameters. The following group of Eqs. (10–17) given below are formed, which shows the relationship equations between L_1, W_1, L_2, W_2 to BW and FR.

BW for L_1-

$$BW_1 = -6.3842 \times 10^{-5}L_1^4 + 0.0011L_1^3 + 0.0406L_1^2 \\ + 0.4437L_1 + 7.4043 \tag{10}$$

FR for L_1-

$$FR_1 = 1.1985 \times 10^{-6}L_1^4 - 3.671 \times 10^{-5}L_1^3 - 0.0008L_1^2 \\ + 0.0265L_1 + 2.393 \tag{11}$$

BW for W_1-

$$BW_2 = -0.0018W_1^4 + 0.0126W_1^3 + 0.3565W_1^2 \\ - 2.1557W_1 + 25.9447 \tag{12}$$

FR for W_1-

$$FR_2 = 2.7739 \times 10^{-6}W_1^4 - 0.0006W_1^3 + 0.0038W_1^2 \\ + 0.0198W_1 + 2.4157 \tag{13}$$

BW for L_2-

$$BW_3 = -0.2582L_2^4 + 0.8705L_2^3 + 3.808L_2^2 - 3.9695L_2 \\ + 5.521 \tag{14}$$

FR for L_2-

$$FR_3 = 0.0003L_2^4 - 0.0038L_2^3 - 0.022L_2^2 + 0.1282L_2 \\ + 2.4338 \tag{15}$$

BW for W_2-

$$BW_4 = -0.0182W_2^4 + 0.0522W_2^3 + 0.9775W_2^2 \\ + 2.4367W_2 - 0.9856 \tag{16}$$

FR for W_2-

Table 4 Variable parameter versus return loss, resonant frequency and bandwidth

Parameters variation (Value)	Return loss (dB)	Resonant frequency (GHz)	Bandwidth (BW) (%)
L_1 = 15 mm	− 15.26	2.56	24.95
L_1 = 24 mm	− 16.05	2.52	35.16
L_1 = 25 mm	− 15.49	2.52	34.45
W_1 = 2 mm	− 34.83	2.49	14.89
W_1 = 10 mm	− 13.91	2.55	35.98
W_1 = 14 mm	− 16.57	2.10	33.26
L_2 = 1.8 mm	− 19.41	2.38	36.21
L_2 = 2.2 mm	− 20.73	2.45	38.81
L_2 = 4.2 mm	− 12.09	2.58	15.20
W_2 = 4.2 mm	− 14.94	2.53	25.91
W_2 = 8.2 mm	− 18.55	2.57	37.86
W_2 = 9 mm	− 12.61	2.51	18.55

$$FR_4 = 2.2166 \times 10^{-5}W_2^4 - 0.0006W_2^3 - 0.0031W_2^2 + 0.0902W_2 + 2.2233 \tag{17}$$

7.7 Formation of Fitness Function

The fitness function has been formed by utilizing Root-Mean-Square Error (RMSE)-based fitness function. Eq. (18) given below is used to generate the root-mean-square error E_i of a specific program-i

$$E_i = \sqrt{\left(\frac{1}{n}\right)\sum_{j=1}^{n}\left(P_{ij} - T_j\right)^2} \tag{18}$$

where $E_i = 0$, for perfect fit and all $P_{ij} = T_j$. n = Total fitness cases. P_{ij} = Value predicted by the individual program i for fitness case jth out of all fitness cases. T_j = Target value for fitness case j.

Above fitness Eq. (18) is employed to generate required fitness function as given below (Rajpoot et al. 2014).

$$F(x) = \sqrt{P\left(BW - BW_{target}\right)^2 + Q\left(f_r - f_{rtarget}\right)^2} \tag{19}$$

The parameters P and Q are known as biasing constants. The different values of P and Q control the contribution of each term to overall fitness function. The parameters $f_{rtarget}$ and BW_{targat} are desired resonant frequency (FR) and antenna bandwidth (BW), respectively. By changing the bias constant P, the created PSO optimize the antenna toward the bandwidth (BW) while changing the bias constant Q, PSO optimize the antenna toward resonating frequency (FR) (Islam et al. 2009).

Utilizing the relationship Eqs. (10–17) as given above and RMSE-based fitness function as given in Eq. (19), we composed PSO program in MATLAB and run it. The bias parameter P and Q has been set at three different values as P = 0.9, Q = 0.1; P = 0.8, Q = 0.2 and P = 0.7, Q = 0.3

for giving additional priority to bandwidth enhancement. We obtained three set of optimized values of parameters L_1, W_1, L_2, and W_2 after running 200 iterations and 70 particles. The optimized values (in mm) of L_1 = 20.1522, W_1 = 10.4432, L_2 = 2.9083 and W_2 = 6.5762 for P = 0.9, Q = 0.1; L_1 = 18.1959, W_1 = 9.1497, L_2 = 2.2357 and W_2 = 6.1201 for P = 0.8, Q = 0.2; while L_1 = 18.4235, W_1 = 9.0426, L_2 = 2.4470 and W_2 = 6.8391 for P = 0.7, Q = 0.3. The L-shape slotted antenna again redesigned at above three set of optimized value of parameters and simulated with IE3D tool. The obtained results of three antennas have been recorded and compared with non-optimized L-shape slotted antenna as exhibited in Table 5. For bias parameters P = 0.9 and Q = 0.1, redesigned antenna is resonating at 2.56 GHz between 1.92 and 2.89 GHz exhibiting 40.33% (970 MHz) bandwidth with − 15.68 dB return loss. The bandwidth is increases 30.94% (from 30.8 to 40.33%) and resonant frequency shifted away (from 2.54 to 2.56 GHz) but return loss almost same. Since resonant frequency moved away at 2.56 GHz with respect to design frequency 2.50 GHz, so value of bias parameter Q is increased and set at P = 0.8 and Q = 0.2. The redesigned antenna improved resonant frequency and resonating at 2.52 GHz between 1.89 and 2.91 GHz. The bandwidth of antenna is obtained 42.5% (1020 MHz) with increased return loss of –18.61 dB. Thus, the bandwidth of this antenna is increases 37.98% (from 30.8% to 42.5%). Still, resonant frequency 2.52 GHz have small mismatch with design frequency 2.50 GHz. Now the value of bias parameter Q is further increases and set at P = 0.7 and Q = 0.3. At this time, redesigned antenna is resonating at exactly same frequency at 2.50 GHz between 1.88 and 2.95 GHz as design frequency. Return loss and bandwidth both are improved and obtained − 21.22 dB and 44.31% (1070 MHz), respectively. Thus, redesigned antenna for P = 0.7 and Q = 0.3 at L_1 = 18.4235,

Table 5 Comparison between non-optimized and PSO optimized L-shaped open ended slot antenna

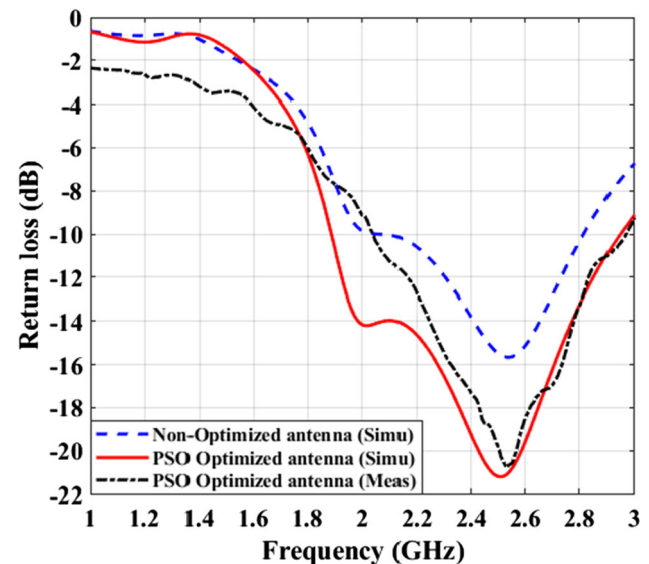| Optimized parameters	Non-optimized L-shaped open ended slot antenna	PSO optimized L-shaped open ended slot antenna		
		$P = 0.9, Q = 0.1$	$P = 0.8, Q = 0.2$	$P = 0.7, Q = 0.3$
L_1 (mm)	20	20.1522	18.1959	18.4235
W_1 (mm)	8	10.4432	9.1497	9.0426
L_2 (mm)	3	2.9083	2.2357	2.4470
W_2 (mm)	5	6.5762	6.1201	6.8391
f_r (GHz)	2.54	2.56	2.52	2.50
Bandwidth (%)	30.8	40.33	42.5	44.31
Return loss (dB)	− 15.67	− 15.68	− 18.61	− 21.22
VSWR	1.39	1.39	1.27	1.24

$W_1 = 9.0426$, $L_2 = 2.4470$ and $W_2 = 6.8391$ is considered as PSO optimized L-shaped open ended slot antenna with increased bandwidth of 43.86% (from 30.8 to 44.31%) resonating at exactly design frequency 2.50 GHz. The comparative analysis and return loss plot for different values of P and Q are exhibited in Table 5 and Fig. 7, respectively. From Table 5, it can be observed that variable parameters W_1 and W_2 both are increases from their initial values 8 mm and 5 mm to 9.0426 mm and 6.8391 mm respectively while L_1 and L_2 are decreases from their initial values 20 mm and 3 mm to 18.4235 mm and 2.4470, respectively. The geometry of PSO optimized L-shaped open ended slot antenna designed at optimized value $L_1 = 18.42$ mm, $W_1 = 9.04$ mm, $L_2 = 2.45$ mm and $W_2 = 6.84$ mm has been exhibited in Figs. 2a and 3c.
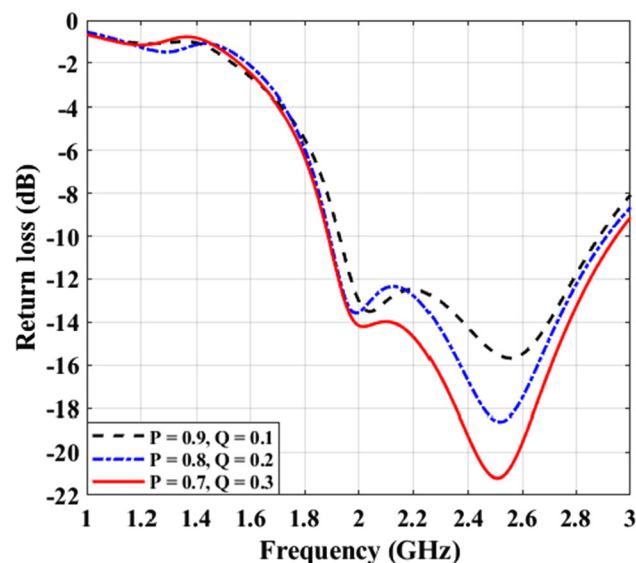
Table 6 Performance comparison of measured and simulation antenna

Parameter	Simulated	Measured
Impedance bandwidth (%)	44.31 (1070 MHz)	37.6 (940 MHz)
Return loss (dB)	− 21.22	− 20.81
Frequency range (GHz)	1.88–2.95	2.03–2.97
Resonant frequency (GHz)	2.50	2.53
Gain (dB)	3.3	3.5

8 Results and Discussion

The fractional bandwidth of PSO optimized L-shaped open ended slot antenna is enhanced from 30.8 (750 MHz) to 44.31% (1070 MHz) and resonating at exactly design frequency 2.50 GHz with − 21.22 dB return loss. The

Fig. 7 Comparative return loss plot for different values of P and Q

Fig. 8 Comparative return loss graph of simulated and measured non-optimized and PSO optimized L-shaped slot open ended antenna
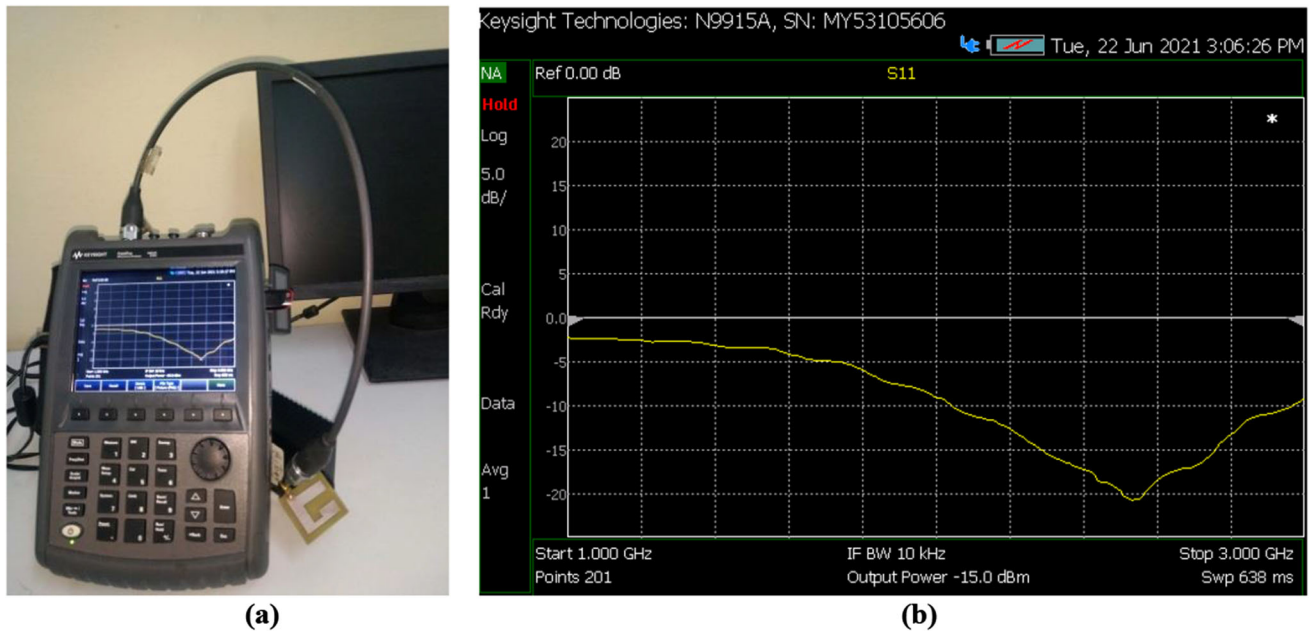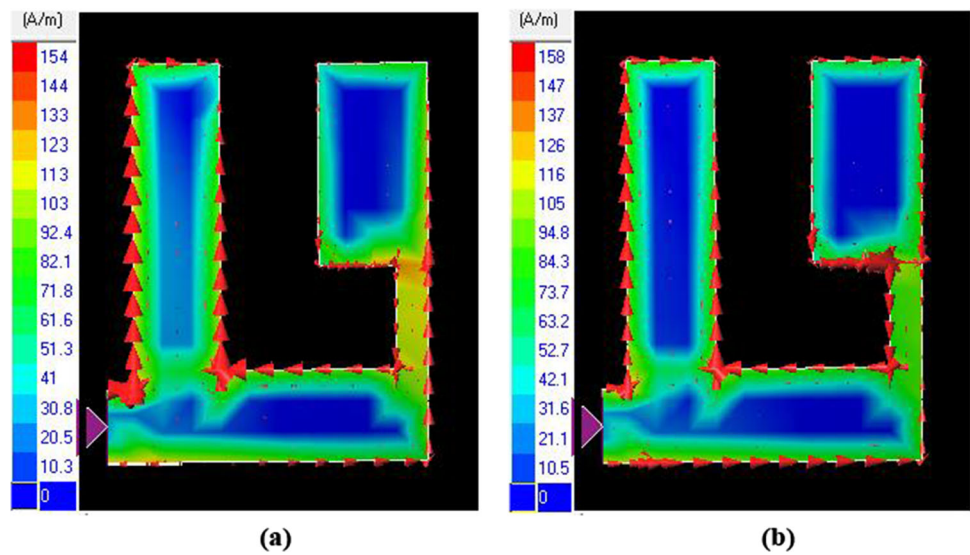
Fig. 9 Image measured by VNA **a** Measurement setup **b** Measured return loss graph

**Fig. 10** Surface current density of proposed antenna at frequencies **a** 2.0 GHz **b** 2.50 GHz

optimized antenna is resonating between lower frequency 1.88 GHz and higher frequency 2.95 GHz. From Table 6, it can be seen that bandwidth, VSWR and return loss of the optimized L-shaped open ended slot antenna have been improved as compared to non-optimized L-shaped slot antenna. Return loss, radiation pattern, surface current density, gain, efficiency and directivity of optimized L-shaped open ended slot antenna are analyzed at resonant frequency 2.50 GHz and plotted for frequency range 1–3 GHz. Comparative simulated return loss plot of optimized and non-optimized L-shaped open ended slot

antenna along with experimentally measured return loss have been exhibited in Fig. 8.

VSWR value for both non-optimized and PSO optimized L-shaped open ended slot antennas are below 2 for overall resonating band. Smaller VSWR value shows that the designed antenna matches the transmission line more appropriately and the antenna transmit higher radiation power. The simulated VSWR of non-optimized and PSO optimized L-shaped open ended slot antenna are 1.39 and 1.24 respectively at their resonant frequency 2.54 GHz and 2.50 GHz which is considerable. Conventional and non-
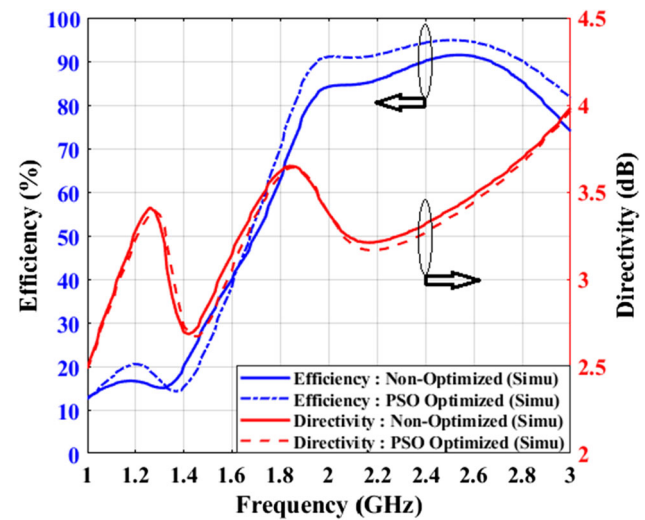
Fig. 11 Simulated and measured E-plane (x–z plane) and H-plane (x–y plane) radiation pattern of optimized antenna at frequencies **a** 2.0 GHz **b** 2.50 GHz

(a)

(b)
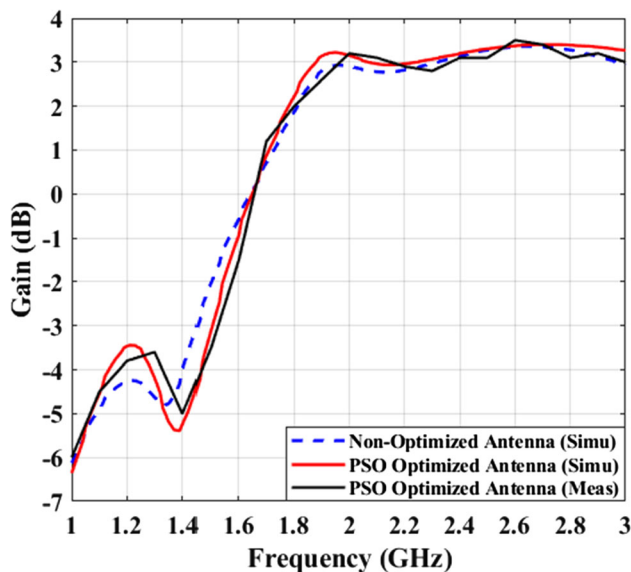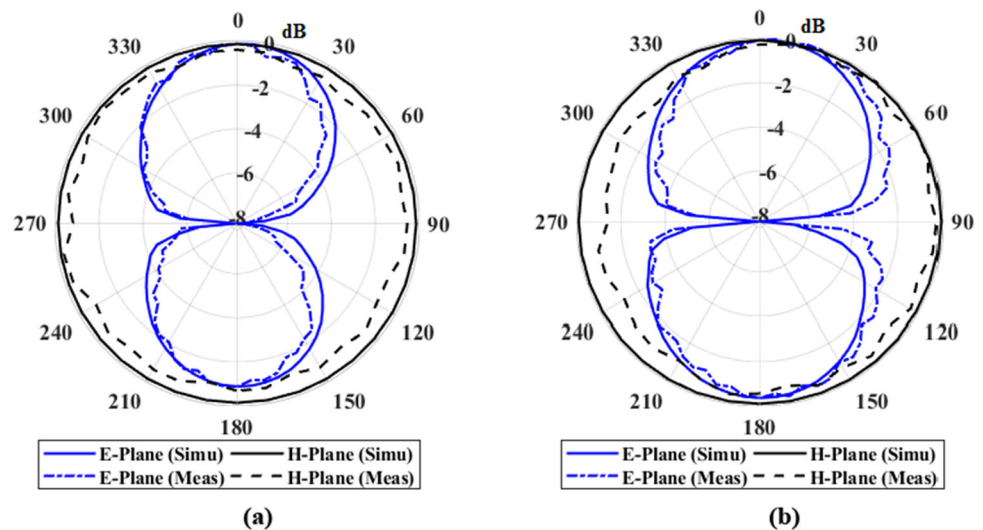
Fig. 12 Gain Versus frequency graph of non-optimized and PSO optimized L-shaped open ended slot antenna

Fig. 13 Efficiency and directivity graph of non-optimized and PSO optimized L-shaped open ended slot antenna

optimized antennas have simulated input impedance $Z = 33.5 – j9.3\ \Omega$ ($|Z| = 33.8\ \Omega$) and $Z = 62.9 + j13.5\ \Omega$ ($|Z| = 64.3\ \Omega$) at 2.44 GHz and 2.54 GHz resonant frequency, respectively. However, the simulated input impedance of PSO optimized L-shaped open ended slot antenna is $Z = 53.5 + j10.7\ \Omega$ ($|Z| = 54.6\Omega$) at 2.50 GHz resonant frequency. Since proposed antenna is excited by characteristic impedance of 50Ω line feed. Thus, PSO optimized antenna exhibits good impedance matching with feed line showing a small mismatch of only 4.6 Ω in magnitude at 2.50 GHz.

Fabricated antenna design (front view and back view) at optimized value of parameters have been exhibited in

Fig. 2c and d, respectively. The measurement of optimized L-shape slotted antenna has been performed by VNA (Vector network analyzer) and anechoic chamber. The comparative performance investigation of simulated and measured antenna has been exhibited in Table 6. The measured impedance bandwidth of proposed PSO optimized L-shaped open ended slot antenna is achieved 37.6% (940 MHz) between frequency ranges 2.03–2.97 GHz with return loss of − 20.81 dB at resonant frequency 2.53 GHz. The simulation result obtained by IE3D and experimental result measured by network analyzer vary due to improper feed line connection and fabrication (etching) defects. A small mismatch (deviation) of 6.71% (130 MHz), − 0.41 dB and 0.03 GHz has been observed between simulated and measured bandwidth, return loss and resonant frequency, respectively. However, the achieved

Table 7 Performance comparison between optimized antenna and single band reported reference antennas

References	Antenna size	Operating range (GHz)	Resonant Freq.(GHz)	Bandwidth (%)	Application
Jin and Samii (2005)	$0.37 \times 0.37 = 0.14\ \lambda_0^2$	1.79–2.43	1.85	30.5% (640 MHz)	RFID/WLAN
Islam et al. (2009)	$0.57 \times 0.38 = 0.22\ \lambda_0^2$	NR	2.16	32.56% (700 MHz)	IMT-2000
Behera and Choukiker (2010)	$0.32 \times 0.39 = 0.13\ \lambda_0^2$	2.384–2.417	2.4	1.37% (33.54 MHz)	WLAN
Choukiker et al. (2011)	$0.3 \times 0.54 = 0.16\ \lambda_0^2$	2.40–2.52	2.42	4.88% (121.9 MHz	ISM band
Tiang et al. (2014)	$0.89 \times 0.89 = 0.79\ \lambda_0^2$	NR	2.47	2.73% (67.5 MHz)	WLAN
Rajpoot et al. (2014)	$0.32 \times 0.39 = 0.13\ \lambda_0^2$	1.65–2.62	2.41	45.72% (970 MHz)	WLAN
Tang et al. (2018)	0.14 (radi) $= 0.06\ \lambda_0^2$	0.666–0.797	0.7	17.97% (131.5 MHz)	Wireless
Neyestanak et al. (2007)	$0.44 \times 0.31 = 0.14\ \lambda_0^2$	1.8–2.6	1.88/2.37	36.7% (800 MHz)	RFID/WLAN
Kamakshi et al. (2014)	$0.74 \times 0.49 = 0.36\ \lambda_0^2$	1.56–2.12	1.84	30.5% (560 MHz)	Broadband
He et al. (2015)	$0.33 \times 0.33 = 0.11\ \lambda_0^2$	1.09–1.51	1.3	32.1% (420 MHz)	Broadband
Zhang et al. (2016)	$0.72 \times 0.72 = 0.52\ \lambda_0^2$	2.29–2.94	2.45	24.8% (650 MHz)	WLAN/WiMAX
Sukur et al. (2016)	$0.34 \times 0.34 = 0.12\ \lambda_0^2$	0.92–1.33	1.13	36.44% (410 MHz)	RFID
Proposed antenna	$0.32 \times 0.38 = 0.12\ \lambda_0^2$	1.88–2.95	2.50	44.31% (1070 MHz)	WLAN/WiMAX

NR, not reported (Value is not given in article)

Fig. 14 Antenna size and bandwidth comparison of reported antennas with proposed antenna
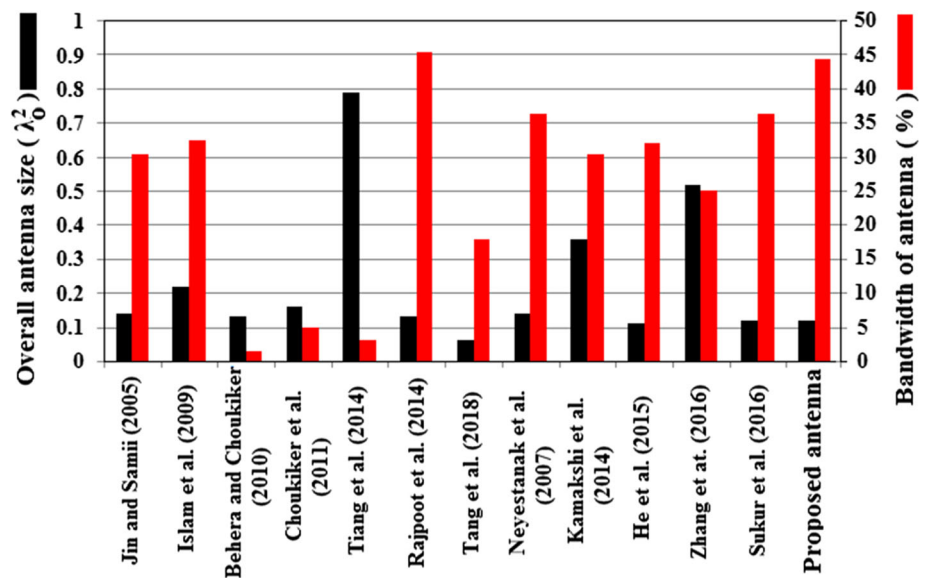
bandwidth is admissible to meet the requirements of WLAN and WiMAX utilization. The measurement setup photograph and return loss graph measured by network analyzer has been exhibited in Fig. 9a and b respectively.

Figure 10a and b shows the surface current distribution of proposed optimized L-shaped open ended slot antenna at frequency 2.0 GHz and 2.50 GHz, respectively. Peak surface current distribution are 154(A/m) and 158(A/m) at frequency 2.0 GHz and 2.50 GHz, respectively. The strength of surface current density at 2.0 GHz frequency is high near left vertical arm of patch while it is decreases at

2.50 GHz frequency. Near bottom edge of patch at 2.0 GHz frequency, strength of surface current is weak while it increases at 2.50 GHz frequency. Figure 11a and b shows the simulated and measured radiation pattern in E-plane and H-plane of proposed PSO optimized L-shaped open ended slot antenna at frequency 2.0 GHz and 2.50 GHz, respectively. Both simulated and measured radiation pattern in E-plane are bi-directional while omnidirectional in H-plane at both frequencies. 3 dB beam width of proposed PSO optimized L- shaped open ended

slot antenna is 80.86° (66.48°, 147.34°) at resonant frequency 2.50 GHz.

From Fig. 12, it can see that, peak gain of simulated non-optimized and proposed PSO optimized L-shaped open ended slot antenna are almost same and it is 3.3 dB at 2.54 GHz and 2.50 GHz resonant frequency. But the measured gain at frequency 2.50 GHz is 3.1 dB and maximum gain is 3.5 dB at frequency 2.6 GHz for optimized antenna. As exhibited in Fig. 13, the simulated efficiency of antenna are 91.4% and 94.8% while simulated directivity are 3.432 dB and 3.364 dB for non-optimized and proposed PSO optimized L-shaped open ended slot antenna at 2.54 GHz and 2.50 GHz resonant frequency, respectively. Non-optimized antenna shows antenna efficiency more than 84% while PSO optimized L-shaped open ended slot antenna shows more than 85% in overall resonating band.

A comparative study of proposed optimized antenna in terms of electrical size of antenna, operating band range, resonant frequency and bandwidth have been discussed with recently published reported reference antennas based on PSO and other optimization shown in Table 7. However, the comparison of overall antenna size of proposed optimized antenna with reported reference antennas using bar graph has been shown in Fig. 14. The presented optimized antenna has compact overall size (0.12 λ_0^2) and large bandwidth of 44.31% (1070 MHz). From Table 7 and Fig. 14, it can be noticed that antennas (Jin and Samii 2005) (0.14 λ_0^2), (Islam et al. 2009) (0.22 λ_0^2), (Behera and Choukiker 2010) (0.13 λ_0^2), (Choukiker et al. 2011) (0.16 λ_0^2), (Rajpoot et al. 2014) (0.13 λ_0^2) and (Neyestanak et al. 2007) (0.14 λ_0^2) have large antenna size (area) compared to proposed optimized antenna (0.12 λ_0^2) with a factor of 1.17, 1.83, 1.08, 1.33, 1.08 and 1.17, respectively. The reference antenna (Kamakshi et al. 2014) (0.36 λ_0^2) has large overall size exactly triple time while reported reference antennas (Zhang et al. 2016) (0.52 λ_0^2) and (Tiang et al. 2014) (0.79 λ_0^2) have very large overall size more than four and six times with factor of 4.33 and 6.58, respectively. Only reference antenna (Sukur et al. 2016) (0.12 λ_0^2) has equal overall size as proposed antenna. However, only two reference antennas (Tang et al. 2018) (0.06 λ_0^2) and (He et al. 2015) (0.11 λ_0^2) have relatively small overall size with factor of 0.5 and 0.92, respectively.

Figure 14 also represents the comparative investigation in terms of impedance bandwidth of proposed optimized L-shaped open ended slot antenna with reported antenna references for 0.5 GHz to 3 GHz applications. From Fig. 14 and Table 7, it can also be observed that the bandwidth ($S_{11} < -10$ dB) of proposed optimized antenna 44.31% (1070 MHz) is larger than reported antennas (Neyestanak et al. 2007) (36.7%) and (Sukur et al. 2016) (36.44%) by small difference of 7.61% and 7.75%, respectively. The reported antennas (Jin and Samii 2005) (30.5%), (Islam et al. 2009) (32.56%), (Kamakshi et al. 2014) (30.5%), (He et al. 2015) (32.1%) and (Zhang et al. 2016) (24.8%) have narrow bandwidth by difference of 13.81%, 11.75%, 13.81%, 12.21% and 19.51%, respectively. However, four other reported antennas (Behera and Choukiker 2010) (1.37%), (Choukiker et al. 2011) (4.88%), (Tiang et al. 2014) (2.73%) and (Tang et al. 2018) (17.97%), also have narrow bandwidth by large difference of 42.94%, 39.43%, 41.58% and 26.34%, respectively. Only reference antenna (Rajpoot et al. 2014) (45.72%) has slightly large bandwidth by difference of 1.41%.

9 Conclusion

The design, parametric analysis and optimization of antenna has been presented and analyzed. The PSO-based optimized antenna is designed and constructed to overcome the restriction of limited bandwidth of ordinary patch antenna. The proposed article investigates the bandwidth optimization of antenna design effort to expand the bandwidth and fix the resonant frequency exactly at design frequency 2.50 GHz. In this work, curve fitting based PSO algorithm has been written with utilizing relationship equations achieved by different parameters. Applying PSO program, the bandwidth of L-shaped open ended slot antenna has been increased by 43.86% from 30.8 to 44.31% with resonant frequency 2.50 GHz applicable in WLAN/WiMAX communication. It has been realized that being as a stochastic global optimizer, PSO is particularly appropriate for the optimizations of antenna design which are usually extremely nonlinear. PSO optimized L-shaped open ended slot antenna has peak gain of 3.3 dB and VSWR of 1.24 at resonant frequency 2.50 GHz.

Declarations

Conflict of interest The authors declare that they have no conflict of interest.

References

Aneesh M, Ansari JA, Singh A, Kamakshi SSS (2013) Analysis of S-shape microstrip patch antenna for bluetooth application. Int J Sci Res Publ 3(11):1–4

Balanis CA (2005) Antenna theory analysis and design. Wiley, New York

Behera SK, Choukiker Y (2010) Design and optimization of dual band microstrip antenna using particle swarm optimization technique. J Infrared Millimeter Terahertz Waves 31(11):1346–1354

Choukiker YK, Behera SK, Pandey BK, Jyoti R (2011) Optimization of planar antenna for ISM band using particle swarm optimization technique. Int J Microw Opt Technol 6(3):124–129

Dey S, Sinha A, Gill B, Gangopadhyaya M, Ray S (2016) Resonant frequency optimization of rectangular gap coupled microstrip antenna using particle swarm optimization algorithm. In: IEEE Conference, pp 1–4

Graphmatica software by Keith Hertzer Copyright © 1992–2014 kSoft, Version 2.4.2.1

Gupta N, Saxena J, Bhatia KS (2020) Optimized metamaterial-loaded fractal antenna using modified hybrid BF-PSO algorithm. Neural Comput Appl 32:7153–7169

He M, Ye X, Zhou P, Zhao G, Zhang C, Sun H (2015) A small-size dual-feed broadband circularly polarized U-slot patch antenna. IEEE Antennas Wirel Propag Lett 14:898–901

Islam MT, Misran N, Take TC, Moniruzzaman M (2009) Optimization of microstrip patch antenna using particle swarm optimization with curve fitting. In: Proceedings of international conference on electrical engineering and informatics, Selangor, Malaysia, pp 711–714

Jin N, Samii YR (2005) Parallel particle swarm optimization and finite- difference time-domain (PSO/FDTD) algorithm for multiband and wide-band patch antenna designs. IEEE Trans Antennas Propag 53(11):3459–3468

Kamakshi K, Singh A, Aneesh M, Ansari JA (2014) Novel design of microstrip antenna with improved bandwidth. Int J Microw Sci Technol. https://doi.org/10.1155/2014/659592

Kaur G, Rattan M, Jain C (2017a) Optimization of swastika slotted fractal antenna using genetic algorithm and bat algorithm for S-band utilities. Wirel Pers Commun 97:95–107

Kaur G, Rattan M, Jain C (2017b) Design and optimization of PSI (Ψ) slotted fractal antenna using ANN and GA for multiband applications. Wirel Pers Commun 97:4573–4585

Kennedy J, Eberhart R (1995) Particle swarm optimization. Proc IEEE Int Conf Neural Netw 4:1942–1948

Kibria S, Islam MT, Yatim B, Azim R (2014) A modified PSO technique using heterogeneous boundary conditions for broad band compact microstrip antenna designing. Ann Telecommun 69:509–514

MATLAB and Simulink Version (2014a)

Neyestanak AAL, Kashani FH, Barkeshli K (2007) W-shaped enhanced-bandwidth patch antenna for wireless communication. Wirel Pers Commun 43:1257–1265

Rajpoot V, Srivastava DK, Saurabh AK (2014) Optimization of I-shape microstrip patch antenna using PSO and curve fitting. J Comput Electron 13(4):1010–1013

Sukur MIA, Rahim MKA, Murad NA (2016) Bandwidth enhancement of rectangular dielectric resonator antenna using circular slot coupled technique. Microw Opt Technol Lett 58(3):505–509

Sun L, Hu J, Hu K, He M, Chen H (2016) Multi-species particle swarms optimization based on orthogonal learning and its application for optimal design of a butterfly-shaped patch antenna. J Central South Univ 23:2048–2062

Sun C, Wu Z, Bai B (2017) A novel compact wideband patch antenna for GNSS application. IEEE Trans Antennas Propag 65(12):7334–7339

Tang MC, Chen X, Li M, Ziolkowski RW (2018) Particle swarm optimized, 3D-printed, wideband, compact hemispherical antenna. IEEE Antennas Wirel Propag Lett 17(11):2031–2035

Tiang J, Islam MT, Misran N, Singh MJ (2014) Design of a dual-band microstrip antenna using particle swarm optimization with curve fitting. Ann Telecommun 69:633–640

Verma RK, Srivastava DK (2020) Design and analysis of triple-band rectangular microstrip antenna loaded with notches and slots for wireless applications. Wirel Pers Commun 114(2):1847–2186

Wang HY, Lancaster MJ (1999) Aperture-coupled thin film superconducting meander antennas. IEEE Trans Antennas Propag 47(5):829–836

Zeland Software Inc. (2012) 'IE3D' Electromagnetic simulation and optimization package, Version 12.00

Zhang J, Lu WJ, Li L, Zhu L, Zhu HB (2016) Wideband dual-mode planar endfire antenna with circular polarisation. Electron Lett 52(12):1000–1001